

CFD STUDY OF SHIP-TO-BANK INTERACTION

(DOI No: 10.3940/rina.ijme.2017.a3.426)

Y K Kim, Lloyd's Register Global Technology Centre, Singapore and **E Y K Ng**, School of Mechanical & Aerospace Engineering, Nanyang Technological University, Singapore

SUMMARY

Ship-to-bank interaction is a complex physical phenomenon that involves not only in the asymmetric pressure field near banks or channels but also shallow water effect. Traditionally many experimental studies were carried out in this field. As numerical method is getting popular, there were various computational approaches as well. In this study, flow around a container ship in confined water is investigated with the open source CFD (Computational Fluid Dynamics) toolbox, OpenFOAM. Computations with several bank arrangements and different settings are performed. The OpenFOAM results are also compared to experiment results for validation.

NOMENCLATURE

| | |
|----------|--|
| P | Pressure (N m^{-2}) |
| F_x | Longitudinal force / Resistance (N) |
| F_y | Transverse force / Sway force (N) |
| g | Acceleration of gravity (m s^{-2}) |
| k | Turbulence kinetic energy ($\text{m}^2 \text{s}^{-2}$) |
| p^* | Dynamic pressure $\text{kg}/(\text{m} \cdot \text{s}^2)$ |
| t | time (s) |
| U | Speed vector (m s^{-1}) |
| w | Artificial velocity normal to the interface of volume fraction (m s^{-1}) |
| M_z | Yaw moment (N m) |
| y_B | Distance from bank wall to the centreline of ship (m) |
| y^+ | Non-dimensional distance from the wall to the first grid point |
| α | Scalar field of volume fraction |
| κ | Surface curvature (m^{-1}) |
| μ | Dynamic viscosity ($\text{kg m}^{-1} \text{s}^{-1}$) |
| ρ | Density of fluid (kg m^{-3}) |
| σ | Surface tension coefficient (N m^{-1}) |
| ω | Specific turbulence dissipation rate (s^{-1}) |
| CFD | Computational Fluid Dynamics |
| RANS | Reynolds Averaged Navier Stokes |
| SST | Shear Stress Transport |
| VOF | Volume of Fluid |

1. INTRODUCTION

When a ship navigates in the proximity of banks or harbours, the pressure field near the ship becomes asymmetric and ship experiences repelling or attracting forces. It makes hard for the ship to manoeuvre and can lead to an accident. In such cases, it is advised to travel at the middle of water to minimise any interaction from the bank or the harbour. However, as this is not always possible, it is important to understand the phenomenon to prevent any dangerous situation. Basically ship-to-bank interaction causes sway force and yaw moment on the ship when separation from the bank wall is small. Moreover, small under keel clearance in confined water allows the interaction even stronger due to the shallow water effect. In addition, there are several other factors

such as propeller effect and bank shape that contribute to the bank effect. Because ships have been increased in size and length in recent years, the importance of prediction and understanding of ship-to-bank interaction are thus getting more critical.

Nowadays, ship-handling simulators play an important role in training captains and crew for safe operation and preventing from accidents. In the mathematical model of the ship-handling simulator, various forces and moments that arise from hull, rudder, propeller, wind, wave, bank effect, etc have to be carefully modelled for realistic simulations. The best way to obtain those forces and moments is to carry out model tests. Captive model test such as HPMM (Horizontal Planar Motion Mechanism) test enables measuring of each force and moment components. However, the test is costly and time consuming. Therefore, it is normal to use empirical methods that are based on the regression formulas from database to estimate these forces and moments. When the accuracy is concerned, CFD (Computational Fluid Dynamics) analysis can give better accuracy to predict those forces and moments. Nowadays, it is not much to say that CFD technology became essential in marine industry. As CFD methodology is being developed, the accuracy and reliability of CFD analysis are also getting better. There were many studies to calculate hydrodynamic forces and moments of mathematical model in ship-handling simulator using CFD approach. In this study, it is decided to work on an open source CFD code to analyse ship-to-bank interaction from various bank arrangements and compare them to the experiment results.

In early days, many experimental studies have been carried out to investigate ship-to-bank interaction and researchers developed empirical formulas that could predict ship-to-bank interaction. It was found that sway force and yaw moment vary in proportion to the square of ship speed. Based on this finding, empirical formulas were suggested from model test results (Norrbin, 1974).

Li *et al.* (2001) found ship-to-bank interaction occurs in a more complex manner. The study suggested there is a point where the sway force is switched from suction to

repulsive force when under keel clearance is extremely small, approximately at about 10% of water draught. Moreover, unlike the study in early times, it turns out that the sway force tends to increase in a higher order than two with respect to the ship speed when under keel clearance is very small. Even in some cases, it became more than order of two at 40% of under keel clearance. At a sloped bank with 30 degrees angle, it tends to reduce force and moments at low speeds but bank effects increase at high speeds as compared to a vertical bank at a low under keel clearance. Moreover, a suction force arises from a rotating propeller compared to the cases without propeller according to the experiments. It was found the more propeller loading caused the larger contribution of suction force.

Expansive shallow water tank tests were carried out at FHR (Flanders Hydraulics Research) in Belgium (Lataire *et al.*, 2009). More than 10,000 model tests of the bank effect were performed and many factors that influence the bank effect were investigated. Through the experiments, it was confirmed that there is a transition point from attraction sway force to repulsion force in shallow water. Small difference from the test results of Li *et al.* (2001) is that the transition happened at slightly higher under keel clearance which is in range of 15% to 20%. Therefore, it is understood that the transition from attraction to repulsion force appears at the under keel clearance of 10–20% water draught. The test results also indicated that propeller action increased the bank effect. Similarly to the results of Li *et al.* (2001), propeller action changed repulsion force into suction force in shallow water where under keel clearance is less than 35% of water draught. These tests results are also developed into empirical formulas. Several sets of test data are made available for the bench marking purpose of simulation model (Lataire *et al.*, 2009). These open test results are used for the validation the CFD calculations in this study.

As numerical technique was being developed, there were many computational studies on the bank effect. In early times, numerical method based on potential theory was used to evaluate the bank effect. When the free surface condition is linearised by double model solution, it was good enough to show qualitative predictions only when the draught and water depth ratio is not too small, such that the ratio is greater than 1.5 (Q. Miao and J. Xia, 2003 and Lee and Lee, 2008). When non-linear boundary condition is applied, panel method was also able to calculate ship-to-bank interaction in extreme shallow water with qualitative agreement (Park *et al.*, 2014). With this non-linear potential method, even the transition point from suction force to repulsion force was found at 40% of the draught-water depth ratio which is slightly higher than the experiment results reported by Li *et al.* (2001) and Lataire *et al.* (2009).

As computational capability is rapidly improving, RANS based finite volume methods were also getting popular.

However, it was quite recent that RANS based method was started to be used in this topic.

Lo *et al.* (2009) carried out transient analysis on the bank effect. Trajectory of a containership travelling near the bank was illustrated. Sway force and yaw moment with time variations at various velocities were calculated at about 30% of the draught-water depth ratio. However, there was no comparison with experiment result.

Wang *et al.* (2010) studied viscous analysis around series 60 hull with $k-\omega$ SST turbulence model from 50% to 1000% of the water depth – draught ratio and showed good agreement with experiments in sway forces but over prediction with the very short distance to the bank wall.

Zou *et al.* (2011) used validation and verification method including a grid convergence study to evaluate RANS based CFD prediction of ship-to-bank interaction. The bank effect between KVLCC hull and a sloped bank was analysed with an overlapping grid of structured mesh and $k-\omega$ SST turbulence model. CFD calculations in the comparison with model tests were done at 50%, 35% and even 10% of the draught-water depth ratio. Furthermore, not only sway force and yaw moment but also rolling, sinkage and trim moment were calculated and compared with potential flow analysis. Because sinkage and trim moment did not show big difference between the potential method and CFD calculation result, free surface effect at slow speed is considered to be insignificant for sinkage and trim. In the study, slip boundary condition was applied on the bank wall instead of no slip condition. The rationale for this boundary condition is not clear and the author also states that the boundary condition may not be accurate. The bank effect analysis gave good agreement in tendencies of yaw and roll moments but with under prediction of sway force.

Mehdi *et al.* (2013) carried out simulation of the viscous flow around LNG ship using RANS method with unstructured hybrid mesh and $k-\omega$ turbulence model. Yaw moment was compared with the experiment results at various velocities and distance from a bank wall but sway force results were not presented in their paper. Calculated yaw moments at different distance from the bank wall and 60% of the draught-water depth ratio were compared to the tank test results and showed qualitative agreement with some under prediction.

From the various studies done in the past, it is still a big challenge to use CFD for ship-to-bank interaction analysis with extreme shallow water. Many studies failed to simulate extreme conditions such as 10% of under keel clearance or did not predict bank effect correctly.

Moreover, during the literature review about numerical studies of the bank effect, viscous flow analysis including free surface effect on the bank effect was not found so far. When a ship travels at slow speed, it is no doubt that free surface elevation is not so high and the importance from

free surface might be relatively low. However, it is believed to be worthwhile to carry out viscous flow analysis with free surface for more accurate prediction of the flow near the proximity of banks. It is also expected to see the difference between the analysis with and without free surface.

2. COMPUTATIONAL SETTINGS

2.1 CASE SETTING

Numerical setup for confined water analyses was established according to the experimental setup done by FHR (Lataire *et al.* 2009). The test cases with several bank arrangements and different under keel clearances were chosen for numerical analysis. As found in the experimental research, a 8000TEU container ship in model scale was used for the simulations with a scale ratio of 80. Table 1 is the principle dimension of the model ship.

Table 1: Principle dimension of the model ship

| | |
|--------------------|---|
| Length overall (m) | 4.332 |
| Breadth (m) | 0.530 |
| Draught (m) | 0.149 ~ 0.180 |
| Block Coefficient | 0.65 ~ 0.66 (depending on the draught) |

The solver used for the simulations is *interFoam* which is a solver for transient solutions of two incompressible, isothermal and immiscible fluids using a VOF (volume of fluid) phase-fraction. The governing equations applied in the solver are the continuity equation (1) and momentum equation (2):

$$\nabla \cdot \mathbf{U} = 0 \quad (1)$$

$$\frac{\partial \rho \mathbf{U}}{\partial t} + \nabla \cdot (\rho \mathbf{U} \mathbf{U}) = -\nabla p^* - g \cdot h \nabla \rho + F_s + \nabla \cdot (\mu \nabla \mathbf{U}) + (\nabla \mathbf{U}) \cdot \mu \quad (2)$$

where μ is dynamic viscosity, p^* is the dynamic pressure, g is acceleration of gravity, ρ is density, \mathbf{U} is velocity vector and h is hydrostatic height of the fluid. Hence, first term in the right hand side represents dynamic pressure and second term hydrostatic pressure. F_s is the source momentum of surface tension, which is expressed as;

$$F_s = \sigma \kappa \nabla \alpha \quad (3)$$

where σ represents the surface tension coefficient, κ is the surface curvature and α is volume fraction which is bounded in $0 \leq \alpha \leq 1$ (0 for air and 1 for water). Surface curvature can be modelled as the boundary condition of

wall surfaces by setting the contact angle. In this simulation, surface tension between the interface and walls are neglected because the effect from surface tension is not significant.

To capture the sharp free surface where α is between 0 and 1 from VOF method, OpenFOAM adopts artificial compression velocity (w) to the transport equation of α :

$$\frac{\partial \alpha}{\partial t} + \nabla \cdot (\mathbf{U} \alpha) + \nabla \cdot \{w \alpha (1 - \alpha)\} = 0 \quad (4)$$

The artificial compression does not affect the solution when the volume fraction is either 0 or 1 so that it can be used for the free surface compression.

For the turbulence model, $k-\omega$ SST has been chosen because it is proven in many of marine applications and in the most of past CFD studies in state of the art review by Wang *et al.* (2010), Zou *et al.* (2011) and Mehdi *et al.* (2013).

The coordinate system to describe settings and forces/moments of the simulation is defined as body fixed and right handed system and that is different from the experiment. The origin is located at the amidships, centreline and keel for x , y and z , respectively. Longitudinal axis (x) is towards the bow, transverse axis (y) towards port side and vertical axis (z) upwards. Therefore, positive sway force directs to the outside the bank and yaw moment is positive when the bow is away and the stern towards the bank (Figure 1). The negative heading angle of the case A means that bow of the ship is toward the bank and the stern is away from the bank.

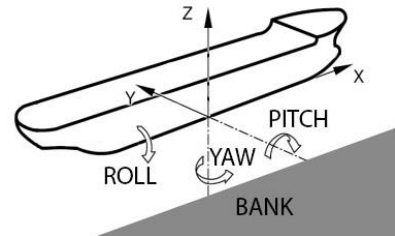


Figure 1: Coordinate system of the CFD simulations

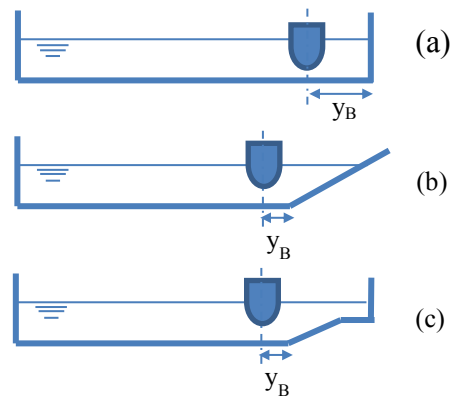


Figure 2: The types of the bank

As can be seen in Figure 2, three types of the banks were used. The arrangement (a) has a straight vertical bank wall. The bank type (b) has an inclined bank wall and type (c) has a bank wall that is inclined and submerged. All three types have 7 meters width.

Three cases were chosen among the experiment results for CFD simulations. Table 2 includes the details of the case arrangements. Under keel clearance from 10% to 100% of the draught and various lateral position of the ship from the bank are included in the test cases. The test cases without propeller thrust have been chosen firstly to see the bank effect merely from asymmetric flow field. If propeller is rotating, it may affect the force and the moment values. In these test cases, propeller was prevented from rotating and there was no thrust. The trim and the sinkage of the ship were not taken into account in the simulation.

Table 2: Test cases without propeller thrust

| Test cases | | A | F | H |
|--------------------------------------|-------|---------|--------|--------|
| Under keel clearance | [%] | 100 | 100 | 10 |
| Draught | [m] | 0.180 | 0.180 | 0.149 |
| Water depth | [m] | 0.360 | 0.360 | 0.163 |
| Forward component of speed vector | [m/s] | 0.6842 | 0.8012 | 0.4578 |
| Transverse component of speed vector | [m/s] | -0.0599 | 0.0 | 0.0 |
| Lateral separation (Y_B) | [m] | 0.265 | 1.435 | 1.965 |
| Heading angle | [deg] | -5.0 | 0.0 | 0.0 |
| Propeller rate | [rpm] | -1 | -1 | -1 |
| Propeller thrust | [N] | -1.10 | -0.93 | -0.37 |
| Propeller torque | [Nmm] | -27.09 | 0.84 | 7.28 |
| Type of bank | - | (b) | (b) | (a) |
| Bank inclination | | 8:1 | 3:1 | 1 |

The case A has slight heading angle with small separation from the bank wall. The case F does not have extreme clearance from the bank wall or the bank bottom, however, the velocity of the ship is relatively high. The case H has very small under keel clearance but moderate distance to the bank wall. Figure 3 is the graphical view of simulations cases without propeller thrust, A, F and H (looking from the forward).

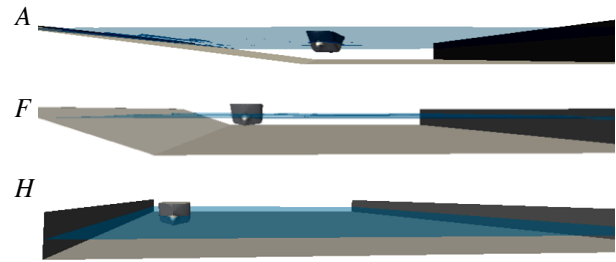


Figure 3: Graphical view of simulation cases

There is a need to understand the contribution of propeller to the bank effect. Although propeller rotation is not modelled in this study, another set of simulations has been compared with the test cases with propeller thrust but without modelling the propeller or thrust in the simulations. This means the ship is simply towed in the simulations to achieve the velocity of the ships but the propeller thrusts and rotations are not modelled. This will indicate the significance of propeller contribution to the bank effect. The purpose of this set of simulations is not to validate the CFD results with the experiment results but to see the contribution of propeller thrust assuming the hypothesis of CFD is realistic enough. They will show the difference as much as propeller rotation contributes to the bank. Table 3 is the detailed experiment conditions of the set of test cases with propeller thrust. The propeller is not modelled in the simulations, hence, propeller thrust is not applied.

Table 3: Test cases with propeller thrust

| Test cases | | D | I | J |
|--------------------------------------|-------|--------|--------|--------|
| Under keel clearance | [%] | 100 | 35 | 100 |
| Draught | [m] | 0.149 | 0.149 | 0.149 |
| Water depth | [m] | 0.297 | 0.200 | 0.297 |
| Forward component of speed vector | [m/s] | 0.6868 | 0.5723 | 0.8012 |
| Transverse component of speed vector | [m/s] | 0.0 | 0.0 | 0.0 |
| Lateral separation | [m] | 1.340 | 0.565 | 0.530 |
| Heading angle | [°] | 0.0 | 0.0 | 0.0 |
| Propeller rate | [rpm] | 540 | 359 | 539 |
| Propeller thrust | [N] | 3.30 | 1.46 | 3.16 |
| Propeller torque | [Nmm] | 53.78 | 20.65 | 62.35 |
| Type of bank | - | (b) | (c) | (c) |
| Bank inclination | | 8:1 | 8:1 | 5:1 |

2.2 SIMULATION MODELLING

Efforts were made to model the mesh finer and prism boundary layers properly because having a certain number of mesh layers would be important in the narrow gap between the bank and the ship as well as in the under keel clearance. The OpenFOAM mesher was prone to fail to generate more than three layers especially on the surface with the big curvature of the hull. The number of the mesh are 0.8~1.4 million for all the cases. The computation domain has been modelled up to the deck height of the ship, however, the deck height is slightly extended to have enough area in the air domain. After some testings, it was found that the freeboard height is sufficient to cover the air domain because the confined water cases have relatively slow speeds.

The mesh size was carefully determined from separate grid independence test in open sea without bank. It was because usual grid dependence tests for the confined water cases were limited due to the small gaps between the hull and the bank. Too fine mesh at the hull surface was not appropriate because it caused y^+ value too small, thus compromising between the cell sizes next to the hull surface and the y^+ value was important for proper modelling of the narrow gap. The meshes were modelled in such a way that y^+ values ranged between 30 and 300 on all the area of the hull surface except the case H due to the narrow gap between the hull and the bank. The more details about the case H will be discussed later. The mesh generation of the single-phase simulations is basically equal to those used for two-phase solver below the water level.

As for the boundary conditions, a fixed value is applied at the inlet for velocity and turbulence properties. At the outlet, zero gradient is applied for velocity and turbulence properties. No slip condition is applied to the hull surface. For the velocity at the bank boundary, the same fixed value with the inlet velocity was used so that no-slip condition can be applied on the bank wall. This is reasonable for no-slip condition on the bank wall of body fixed coordinate system because the point of view is on the ship, and undisturbed water and the bank should have the same velocity. Wall function is applied for k and ω on the ship and the bank wall.

For the single-phase solver, a slip condition is used for the velocity on the top which is free surface level.

3. COMPUTATIONAL RESULT

The numerical results of two-phase solver showed that pressure component dominates over the viscosity with large oscillations. It is presumed that the oscillation is caused from the interaction between the bank and the ship because such oscillation did not appear when the simulation is carried out in open water (using the same settings but in deep water without banks) in spite of relatively slow speed. Even the resistance in x direction revealed much bigger oscillating behaviour compare to

the simulation in open water. Reducing Courant number was also helpful to suppress the oscillation. The average was taken for capturing force and moment values after substantial calculations.

A single-phase steady-state solver *simpleFoam* was tested to compare the result from *interFoam* which is a VOF transient solver. Table 4 is the comparison table of forces and moments between the CFD results and the experiment (Lataire *et al.*, 2009). Comparing the different gradient schemes having 2nd order accuracy, least square generally showed slightly better results compared to Gauss linear. Therefore, the results from least square scheme were presented. *simpleFoam* also allowed good accuracy although they were single-phase simulations without free surface. Least square method also allowed better accuracy for single-phase calculations.

3.1 RESULT SUMMARY

Case A: The two-phase solver over-predicted the F_x and F_y values by 17.8% and 9.8% respectively, but yaw moment suggested good accuracy with 1.4% error. The single-phase solver also showed good accuracy compared to the experiment.

Case F: The two-phase solution gave the good accuracy for longitudinal force and yaw moment, however, sway force was under-predicted by 39%. Single-phase solver predicted better sway force but not for other values.

Table 4: Comparison of the 3 cases (A, F, H) to the experimental results without thrust (Lataire *et al.*, 2009)

| Solver | Force /Moment | A | F | H |
|---------------------------|---------------|--------|--------|-------|
| interFoam (VoF) | $F_x(N)$ | 4.866 | 5.512 | 2.239 |
| | $F_y(N)$ | -5.646 | -1.008 | 1.963 |
| | $M_z(Nm)$ | -9.067 | 1.305 | 5.561 |
| simpleFoam (single-phase) | $F_x(N)$ | 3.922 | 3.794 | 1.880 |
| | $F_y(N)$ | -5.343 | -1.300 | 1.245 |
| | $M_z(Nm)$ | -8.665 | 1.053 | 4.017 |
| EXP | $F_x(N)$ | 4.130 | 5.354 | 2.935 |
| | $F_y(N)$ | -5.139 | -1.648 | 2.545 |
| | $M_z(Nm)$ | -8.939 | 1.804 | 6.959 |

Case H: This case has small under keel clearance which is 10% of water draught, but the separation from the bank wall is however, not small. Unlike the other cases in which the difference was insignificant between two and many prism boundary layers applied near the ship, all the values were under-predicted in this case when two prism layers were used. The details will be discussed in the next section. The values presented in Table 4 were of the

refined mesh with 8 prism boundary layers. F_x represents resistance, F_y sway force and M_z yaw moment.

3.2 UNDER KEEL SPACE MODELLING OF THE CASE H

Because of small under keel clearance of the case H, it was hard to model the mesh in the narrow space properly. If many layers are modelled in the under keel space, y^+ values become too low, i.e. below 30. In that case, the wall function may not be valid. To keep y^+ values bigger than 30, the optimum number of layer in the under keel clearance had to be only about two or three in the case H. The small under keel clearance is known to affect the bank effect significantly, therefore, too few number of layers in the under keel would not be enough to capture the effect. In this case, the best way would be to model y^+ values less than 1 throughout the hull surface and resolve the whole boundary layer without using wall functions. However, this was not successful by the OpenFOAM mesher.

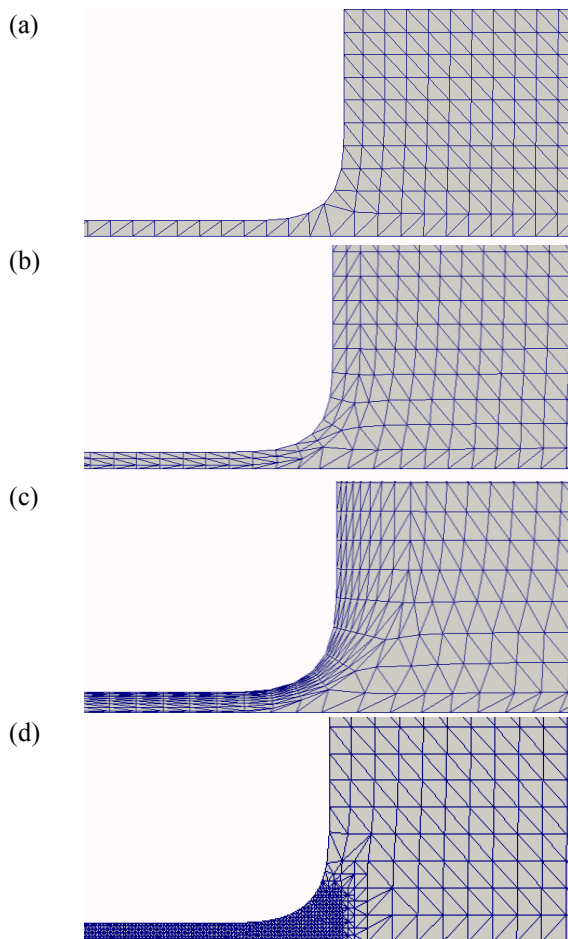


Figure 4: Different meshing of case H with no layer (a), two prism layers (b), eight layers (c) and fine mesh (d)

To compromise between the number of mesh layers and valid y^+ value for the wall function in the under keel space, a comparison has been made. Four different meshes are tested for the case H. They have same mesh

size in other areas but different size in boundary layers or in the under keel space. The tested meshes are shown in Figure 4 as the midship sections near the bilge radius are zoomed in.

Type (a) has no specific modelling for the prism boundary layer, (b) has two prism boundary layers and total three layers in the under keel, (c) has eight prism boundary layers and total nine in the under keel, and (d) has very fine refinement in the under keel clearance without modelling overall boundary layer. The (b) type meshing shows good y^+ distribution to use wall function. Figure 4 illustrates y^+ distribution near the bilge keel area for each of the four meshing type.

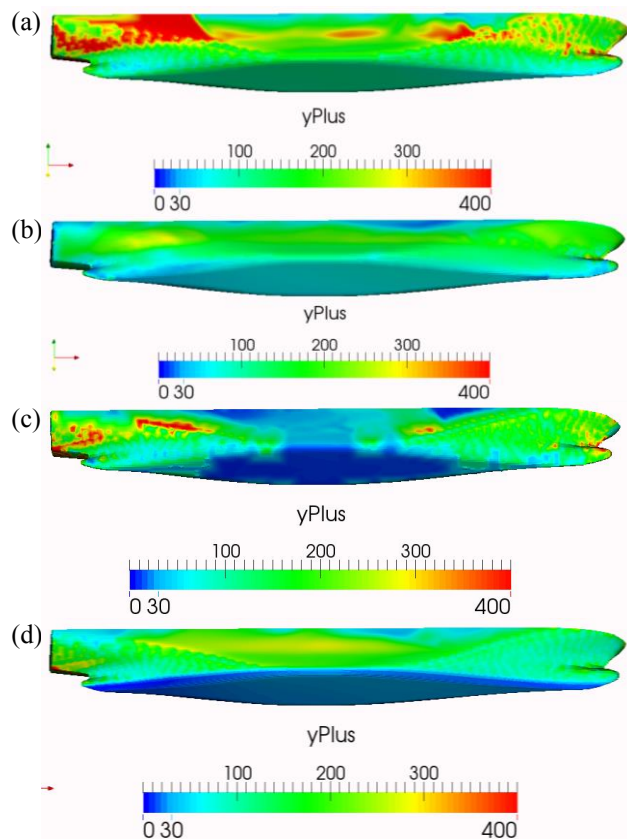


Figure 5: y^+ distribution of the case H with different meshing in the underkeel - no layer (a), two prism layers (b), eight layers (c) and fine mesh in the under keel(d)

Type (a) and (b) have y^+ values above 30 and all are in good range. OpenFOAM mesher has problem when many prism layers have to be created at the boundary layer especially at large curvature. For this reason, it failed to generate complete eight prism layers at fore and aft area of (c) where curvature appears. However, expected number of prism layers has been created in the boundary layer near the parallel middle body where under keel clearance is most significant. This is clearly shown in Figure 5. In (d), very fine mesh was used only in the underkeel space, hence, very low y^+ distribution can be seen on the bottom hull surface. Since majority of area was still modelled with y^+ value above 10 for (d), wall function is applied to all four cases.

Table 5 is the forces and moments from different boundary layer modelling. The (c) type meshing showed the best accuracy in spite of low y^+ distribution at the bottom of the hull. Therefore, it is important to model enough number of prism layers in the under keel clearance to capture the bank effect. Enough number of prism layers at the boundary layer was the most effective modelling. Moreover, the result suggests the importance of under keel clearance modelling. Because (d) shows much better accuracy of sway force than (a), although they have similar cell size at the side wall of the ship.

Table 5: Results with different boundary layer modelling

| | (a) | (b) | (c) | (d) | EXP |
|--------------------|-------|-------|-------|-------|-------|
| No. of mesh (mil.) | 1.11 | 1.13 | 1.15 | 5.21 | - |
| Fx (N) | 1.484 | 2.239 | 2.236 | 2.247 | 2.935 |
| Fy (N) | 0.368 | 1.104 | 1.963 | 1.037 | 2.545 |
| Mz (Nm) | 4.004 | 3.734 | 5.561 | 3.647 | 6.959 |

3.3 COMPARISON OF THE CASES WITH PROPELLER THRUST

Table 6 is the comparison results of the cases (D, I and J) with propeller thrust. Sway forces and yaw moments are compared with the experimental results.

As can be seen in the comparison, when the propeller rotations are not modelled, all the sway forces are under predicted compared to the experiment result. The directions of the sway forces were mostly correct but the magnitudes were all under-estimated. When the ship was towed without propeller thrust in both the simulations and the experiments, the deviation between them was 10%-40%, however, the cases with propeller thrust show at least 2.5 times bigger in suction of sway force than the simulations where the ships were simply towed without propeller thrust. This ascertains propeller loading causes more suction force (Li et al., 2001). Moreover, for the cases with propeller thrust, sway forces were all in suction direction to the bank wall. This is in line with the fact that the propeller rotation either affects the magnitude of sway force or causes suction in sway force (Lataire et al., 2009). However, further comparison of these cases are not reliable but would become speculation, hence, it is not meaningful to discuss further and more study is required to confirm the capability of CFD and the propeller effect. Another limitation is that propeller rotation and the bank locations are all in the same direction in these cases. The predicted yaw moment values indicated reasonable accuracy with the VoF solver even without modelling propeller. For these cases, Gauss linear method provided relatively better results than least square method for both sway force and yaw moment. Single-phase solver showed poor accuracy even for yaw moments.

Table 6: Comparison of the cases (D, I, J) with thrust to the experimental results (Lataire et al., 2009)

| Solver | Force /Moment | D | I | J |
|---------------------------|---------------|--------|--------|--------|
| interFoam (VoF) | Fy (N) | -2.011 | -0.201 | -0.894 |
| | Mz (Nm) | 19.280 | 9.750 | 2.169 |
| simpleFoam (single-phase) | Fy (N) | -2.683 | -1.080 | -1.427 |
| | Mz (Nm) | 4.692 | 1.960 | 1.688 |
| EXP | Fy (N) | -8.056 | -3.682 | -2.264 |
| | Mz (Nm) | 16.407 | 8.312 | 2.065 |

3.4 FREE SURFACE ELEVATION

Free surface elevations were compared with the experimental results. It was measured at three points of the cases F, I and J which are the same in the simulations and the experiments. Table 7 displays the locations of the wave gauges from the centreline of the ship according to the experiment. Wave gauges measure the wave elevation at the defined transverse distances from the centreline of the ship. Figure 6, Figure 7 and Figure 8 are the comparisons of wave elevation with the model test measurement.

Table 7: The locations (m) of the wave gauges with reference to the centreline of the ship (Lataire et al., 2009)

| | Gauge 1 | Gauge 2 | Gauge 3 |
|--------|---------|---------|---------|
| Case F | 0.475 | 1.005 | 1.535 |
| Case I | 0.875 | 1.215 | 2.115 |
| Case J | 0.920 | 1.320 | 1.785 |

The simulations captured the free surface elevation in confined water with reasonable accuracy. The further wave gauges from the ship showed less accuracy of the wave elevation. A steep wave is observed in the case I and it is continued from the hull to the bank wall. This was also found in the experiment but over-predicted in the simulation result at the gauges 1 and 2. In addition, phase delay was observed, especially at the furthest wave gauge from the ship, i.e. wave gauge 3. This phase delay was also found at the gauge 3 of the case F. The phase of wave trough was deviated by about a quarter of trough length. The case J showed relatively good accuracy, however, reason was not found for the better accuracy of the case J compared to the case F and I in terms of the bank arrangement and speed. As the CFD solvers used in these simulations are known to capture free surface elevation quite accurately, the difference in these comparisons is presumed to arise from the under-predicted bank effect that causes asymmetric flow field.

Lastly, the computations did not capture the oscillation of the wave elevation correctly. The experiment showed more oscillation but this was not captured or captured differently in the simulated results.

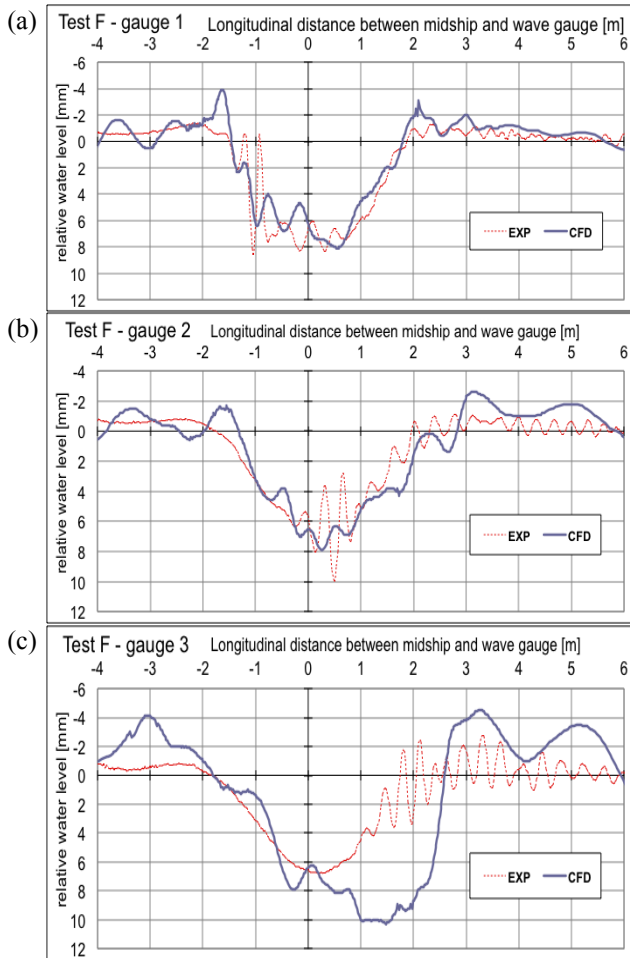


Figure 6: Wave elevation of the case F at (a) gauge 1, (b) gauge 2 and (c) gauge 3 (Lataire *et al.*, 2009)

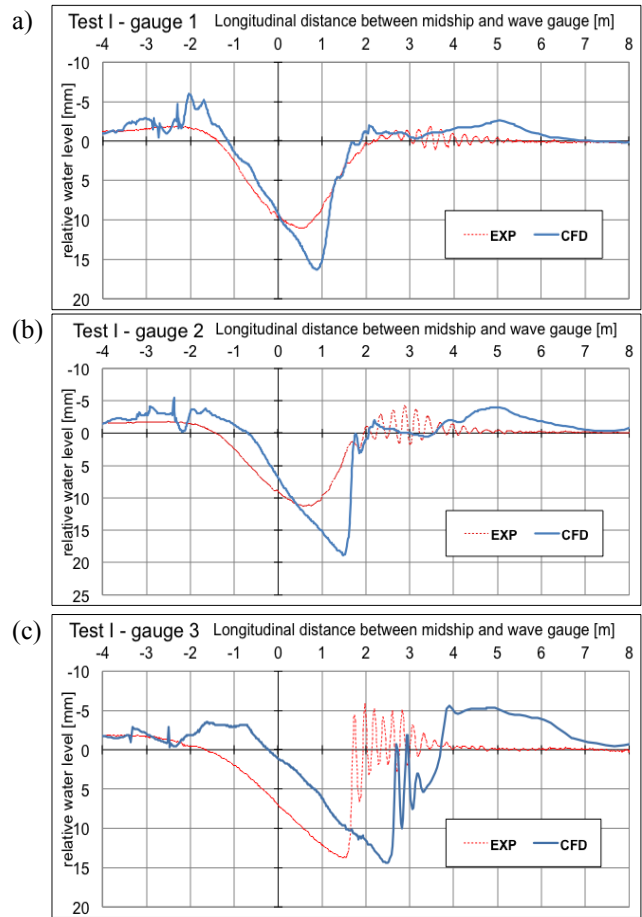


Figure 7: Wave elevation of the case I at (a) gauge 1, (b) gauge 2 and (c) gauge 3 (Lataire *et al.*, 2009)

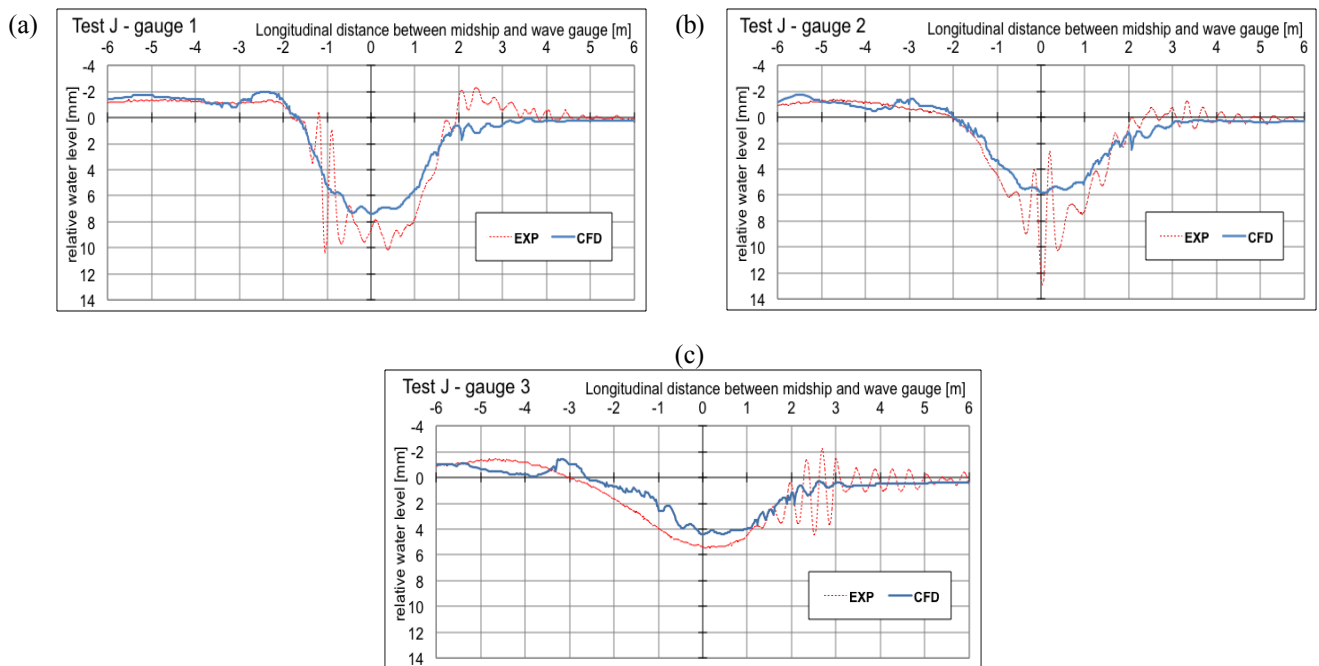


Figure 8: Wave elevation of the case J at (a) gauge 1, (b) gauge 2 and (c) gauge 3 (Lataire *et al.*, 2009)

4. CONCLUSIONS

In this study, flow around a ship in confined water with several bank arrangements was computed by incompressible RANS solvers of OpenFOAM. The results from single-phase and two-phase solver were compared to the experiment result. The hydrodynamic forces and moments due to the bank effect, and wave elevation in confined water were compared to the experimental results. Under keel clearance modelling was evaluated and suggested to compromise between mesh fineness and y^+ distribution.

CFD analysis was good in qualitative prediction of the forces and the moment from bank effect. However, the computation tended to under-predict forces and moment for most of cases. This is most obvious in sway force. These can be led to several reasons. Firstly, there is limitation of meshing in the narrow gap. One thing can be tried is resolving whole boundary layer by modelling y^+ below 1. However, this requires huge computational cost and is hard to achieve with the OpenFOAM mesher. Secondly, fixed heave and pitch motion of CFD calculations could have caused this under-prediction because the two motions were free in the model tests. This assumption of fixed motion neglects squat effect, therefore, better accuracy can be expected if the 2 DOF motions are allowed. However, mesh motion with fine mesh and small keel clearance is a big challenge.

The under-prediction of sway force was more obvious in the cases with propeller rotation although yaw moments were predicted with reasonable accuracy. This explains what experimental study discovered (Li *et al.*, 2001) on how propeller rotation affects the sway force. More study is needed to see whether propeller intervention causes additional sway force to specific direction or affects magnitude of sway force. In this set of experiments, all the cases with propeller rotation resulted in suction forces and the computation without propeller modelling predicted the sway forces to the correct direction but in smaller magnitude. From this comparison, it is noted that propeller rotation seems to affect the magnitude of sway forces but does not give significant contribution to yaw moment. Overall, the calculated sway forces and yaw moments from the bank effect are all in correct directions for all the types of bank shapes and arrangement although ship-to-bank interaction is very complex and difficult to predict the directions.

Free surface elevation was captured reasonably well except the difference in the wave phase. Such a phase delay was more obvious in the case where the water depth is shallow. Less oscillation on the free surface level was observed in the computation than the experimental result. However, from the comparison between the single phase and two phase simulations free surface effect does not give significant contribution. There was no clear improvement of the accuracy of

forces and moment in the bank effect prediction by adding free surface in the CFD simulation. Therefore, single phase solver which is faster and more stable can be useful solution to predict bank effect.

Unfortunately, the experiment results open to the public were only available to limited cases, therefore, systematic parametric study was not possible.

5. REFERENCES

1. LATAIRE, E., VANTORRE, M., LAFORCE, E., ELOOT, K. and DELEFORTRIE G., *Navigation in Confined Waters: Influence of Bank Characteristics on Ship-Bank Interaction*, International Conference on Ship Manoeuvring in Shallow and Confined Water, page 135~143, Antwerp, Belgium, 2007
2. LATAIRE, E., VANTORRE, M. and ELOOT, K., *Systematic Model Tests on Ship-Bank Interaction Effects*, International Conference on Ship Manoeuvring in Shallow and Confined Water: Bank Effect, Antwerp, Belgium, 2009
3. LEE, K. and LEE, S. G., *Investigation of ship maneuvering with hydrodynamic effects between ship and bank*, Journal of Mechanical Science and Technology, No. 22, page 1230~1236, 2008
4. LI, Q., LEER-ANDERSEN, M., OTTOSSON, P. and TRÄGÅRDH, P., *Experimental Investigation of Bank Effects Under Extreme Conditions*, Proceeding of PRADS 2001, page 541-546, Shanghai, China, 2001
5. LO, C., SU, DONG-TAUR and LIN, I-FU, *Applying Computational Fluid Dynamics to Simulate Bank Effects*, 19th International Offshore and Polar Engineering Conference, page 466~471, Osaka, Japan, 2009
6. MIAO, Q., and XIA, J., *Numerical Study of Bank Effect on a Ship Traveling in a Channel*, The 8th International Conference on Numerical Ship Hydrodynamics, Busan, Korea, 2003
7. NAKISA, M., MAIMUN, A., YASSER M. AHMED, SIAN, A.Y., PRIYANTO, A., BEHROUZI, JASWARAMD F., *RANS Simulation of the Viscous Flow around Hull of LNG Ship in Confined Water*, 15th Mathematical and Computational Methods in Science and Engineering, page 133~137, Kuala Lumpur, Malaysia, 2013
8. NORRIBIN, *Bank Effect on a Ship Moving through a Short Dredged Channel*, Proceedings of 10th Symposium on Naval Hydrodynamics, page 71~88, Cambridge, MA, USA, 1974
9. PARK, D. W., CHOI, H. J. and PAIK, K. J., *Bank Effect of a Ship Operating in a Shallow Water and Channel*, Journal of Navigation and Port, Volume 38, No. 1, page 19~27, 2014
10. RUSCHE, H., *Computational Fluid Dynamics of Dispersed Two-phase Flows at High Phase*

- Fractions*, PhD thesis, Imperial College, London, 2002
11. VANTORRE, M., and DELEFORTRIE, G., *Experimental Investigation of Ship-Bank Interaction Forces*, Proceeding of International Conference on Marine Simulation and Ship Manoeuvrability, MARSIM'03, page RC-31-1~9, Kanazawa, Japan, 2003
 12. WANG, H., ZOU, Z., XIE, Y., and KONG, W., *Numerical Study of Viscous Hydrodynamic Forces on a Ship Navigating near Bank in Shallow Water*, Proceedings of the 20th International Offshore and Polar Engineering Conference, page 523~528, Beijing, China, 2010
 13. ZOU L., LARSSON, L., DELEFORTRIE, G. and LATAIRE, E., *CFD Prediction and Validation of Ship-bank Interaction in a Canal*, 2nd International Conference on Ship Manoeuvring in Shallow and Confined Water: Ship to Ship Interaction, May 18-20, Trondheim, Norway, 2011